

Chemotaxis When Bacteria Remember: Drift versus Diffusion

Sakuntala Chatterjee(1), Rava Azeredo da Silveira(2) and Yariv Kafri(1)

(1) *Department of Physics, Technion, Haifa-32000, Israel*

(2) *Department of Physics and Department of Cognitive Studies,
École Normale Supérieure, 24, rue Lhomond, 75005 Paris, France*

Escherichia coli (E. coli) bacteria govern their trajectories by switching between running and tumbling modes as a function of the nutrient concentration they experienced in the past. At short time one observes a drift of the bacterial population, while at long time one observes accumulation in high-nutrient regions. Recent work has pointed to an apparent theoretical contradiction between drift toward favorable regions and accumulation in favorable regions. A number of such earlier studies assume that a bacterium resets its memory at tumbles – a fact not borne out by experiment – and make use of approximate coarse-grained descriptions. Here, we revisit the problem of chemotaxis without resorting to any memory resets. We find that when bacteria respond to the environment in a non-adaptive manner, chemotaxis is generally dominated by diffusion, whereas when bacteria respond in an adaptive manner, chemotaxis is dominated by a bias in the motion. In all cases, the apparent contradiction between favorable drift and favorable accumulation is resolved. We derive our results from detailed simulations and a variety of analytical arguments. In particular, we introduce a new coarse-grained description of chemotaxis as biased diffusion, and we discuss the way it departs from older coarse-grained descriptions.

I. INTRODUCTION

The bacterium *E. coli* moves by switching between two types of motions, termed ‘run’ and ‘tumble’ [1]. Each results from a distinct motion of the flagella. During a run, flagella motors rotate counter clockwise (when looking at the bacteria from the back), inducing an almost constant forward velocity of about $20\mu\text{m}/\text{s}$, along a near-straight line. In an environment with uniform nutrient concentration, run durations are distributed exponentially with a mean value of about $\tau_R = 1\text{s}$ [2]. When motors turn clockwise, the bacterium undergoes a

tumble, during which, to a good approximation, it does not translate but instead changes its direction randomly. In a uniform nutrient-concentration profile, the tumble duration is also distributed exponentially but with a much shorter mean value of about $\tau_T = 0.1s$ [3].

When the nutrient (or, more generally, chemoattractant) concentration varies in space, bacteria tend to accumulate in regions of high concentration [4]. This is achieved by a modulation of both run and tumble durations. The biochemical pathway that controls flagella dynamics is well understood [1, 5–7], and the motion of a single bacterium can be described by a simple stochastic ‘algorithm’ which was measured directly [8, 9]. It represents the motion of the bacterium as a non-Markovian random walker whose stochastic run and tumble durations are modulated via a memory kernel, shown in Fig. 1. Loosely speaking, the kernel compares the nutrient concentration experienced in the recent past with the one experienced in the more distant past. If the difference is positive, the run (tumble) duration is extended (shortened); if it is negative, both run and tumble durations remain unmodulated.

Recent quantitative studies have shown that a simple connection between the stochastic algorithm of motion and the average chemotactic response is far from obvious [10–13]. In particular, these noted that favorable chemotaxis in the steady state was incompatible with a large chemotactic drift velocity towards nutrient rich regions [11, 13]. More specifically, in various approximations, while the negative part of the response kernel was key to favorable accumulation in the steady state, it suppressed the drift velocity. Conversely, the positive part of the response kernel enhanced the drift velocity but reduced the magnitude of the chemotactic response in the steady state.

Here, we carry out a detailed numerical study of the chemotactic behavior of a single bacterium in one dimension without resorting to any of the approximations used in earlier studies. We find that there is no incompatibility between strong steady-state chemotaxis and large drift velocity. A strong steady-state chemotaxis occurs when the positive peak of the response kernel occurs at a time much smaller than τ_R and the negative peak at a time much larger than τ_R , in line with experimental observation. Moreover, we find that the drift velocity is also large in this case.

In order to explain our numerical results, we propose a simple coarse-grained model which describes the bacterium as a biased random walker with a drift velocity and diffusivity, both of which are, in general, position-dependent. This simple model yields good agreement with

results of detailed simulations. We emphasize that our model is distinct from existing coarse-grained descriptions of *E. coli* chemotaxis [14–17]. In these, coarse-graining was performed over left- and right-moving bacteria, separately, after which the two resulting coarse-grained quantities were then added to obtain an equation for the total coarse-grained density. We point out why such approaches can fail and discuss the differences between earlier models and the present coarse-grained model.

II. MATHEMATICAL DESCRIPTION OF BACTERIAL CHEMOTAXIS AND PARADOXES

We begin by discussing our model of chemotaxis and by explaining the above mentioned paradoxes in greater detail. According to the stochastic law of bacterial motion, run durations are Poissonian. A switch from run to tumble occurs during the small time interval between t and $t + dt$ with a probability

$$\frac{dt}{\tau_R} \{1 - \mathcal{F}[c]\}. \quad (1)$$

Here, $\tau_R \simeq 1s$ and $\mathcal{F}[c]$ is a functional of the chemical concentration, $c(t')$, experienced by the bacterium at times $t' \leq t$. Experiments have demonstrated that, in shallow nutrient gradients, the functional can be written in a ‘linear non-linear’ form as

$$\mathcal{F}[c] = \phi(\mathcal{F}_{\text{lin}}) , \quad (2)$$

where

$$\mathcal{F}_{\text{lin}}[c] = \int_{-\infty}^t dt' R(t-t')c(t') \quad (3)$$

and $\phi(\cdot)$ is the threshold-linear function with $\phi(x) = 0$ for $x \leq 0$ and $\phi(x) = x$ for $x > 0$. The functions $\phi(\cdot)$ and $R(t)$ encode the action of the biochemical machinery that processes input signals from the environment. The response kernel, $R(t)$, was investigated experimentally in wild-type bacteria [8, 9]. Measurements yielded a bimodal shape for $R(t)$, with a positive peak around $t \simeq 0.5s$ and a negative peak around $t \simeq 1.5s$ (see Fig. 1). The negative lobe is shallower than the positive one and extends up to $t \simeq 4s$, beyond which it vanishes. To a good approximation the response function satisfies $\int_0^\infty R(t)dt = 0$. The duration of tumbles are modulated in a similar manner: they are Poissonian with a switch probability given by

$$\frac{dt}{\tau_T} \{1 + \mathcal{F}[c]\}. \quad (4)$$

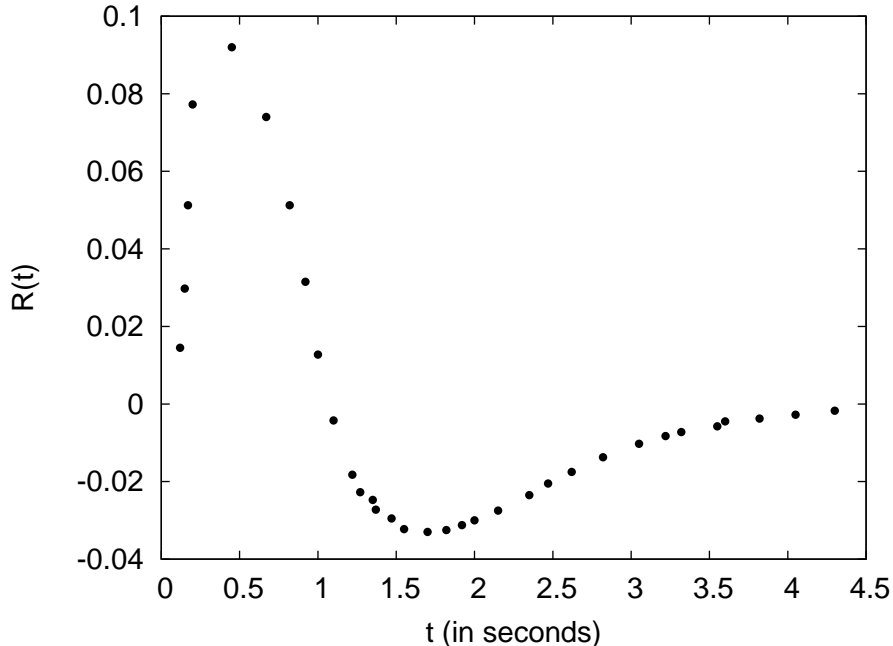


FIG. 1: *Bilobe response function of wild-type E. coli used in the numerics in Figs. 3 and 6. For the sake of computational simplicity, we have used a discrete sampling of the experimental data presented in Ref. [9] instead of working with the complete data set. This did not affect our conclusions.*

Note that $\mathcal{F}[c]$ is the same functional as the one that controls run modulation, defined in Eqs. 2 and 3. Thus, the mathematical problem comes with four characteristic time scales: τ_R , τ_T and the locations of the positive and negative peaks of the response function.

The shape of the response function hints to a simple mechanism for the bacterium to reach regions of high nutrient concentration. The bilobe kernel measures a temporal gradient of the nutrient concentration. According to Eq. 1, if the gradient is positive, runs are extended; if it is negative, runs are unmodulated. However, recent literature [10–12] has pointed out that the connection between this simple picture and a detailed quantitative analysis is tenuous. For example, de Gennes used Eqs. 1 and 4 to calculate the chemotactic drift velocity of bacteria [10]. He found that a singular kernel, $R(t) = \alpha\delta(t - \Delta)$, where δ is a Dirac function and α a positive constant, lead to a mean velocity in the direction of increasing nutrient concentration even when bacteria are memoryless ($\Delta = 0$). Moreover, any addition of a negative contribution to the response kernel, as seen in experiments (see Fig. 1), lowered the drift velocity. Other studies considered the steady-state density profile

of bacteria in a container with closed walls, both in an approximation in which correlations between run durations and probability density were ignored [11] and in an approximation in which the memory of the bacterium was reset at run-to-tumble switches [12]. Both these studies found that, in the steady state, a negative contribution to the response function was mandatory for bacteria to accumulate in regions of high nutrient concentration. These results, together with de Gennes results, seem to indicate that the joint requirement of favorable accumulation in the transient and in the steady-state regimes is incompatible. The paradox was further complicated by the observation [12] that the steady-state single-bacterium probability density was sensitive to the exact shape of the kernel: when the negative part of the kernel was located far beyond τ_R it had little influence on the steady-state distribution [11]. In fact, for kernels similar to the experimental one, model bacteria accumulated in regions with low nutrient concentration in the steady state [12].

III. SIMULATIONS AND ANALYTICAL TREATMENT OF CHEMOTACTIC BACTERIAL ACCUMULATION

In order to resolve these paradoxes and to better understand the mechanism that leads to favorable accumulation of bacteria, we perform careful numerical studies of bacterial motion in one dimension *without* resorting to any of the approximations used previously. In particular, in conformity with experimental observations [8, 9], we do not make any assumption of memory reset at run-to-tumble switches.

We model a bacterium as a one-dimensional non-Markovian random walker. The walker can move either to the left or right with a fixed speed v or it can tumble at a given position before initiating a new run. In this paper, we present results only for the case of instantaneous tumbling with $\tau_T = 0$, while results for non-vanishing τ_T are discussed in the supporting information. There we verify that for adaptive response τ_T does not have any effect on the steady-state density profile. For a non-adaptive response kernel, the correction in the steady-state slope due to finite τ_T is small and proportional to τ_T/τ_R .

The run durations are Poissonian and the probability to tumble is given by Eq. 1. The probability to change the run direction after a tumble is assumed to have a fixed value q , which we treat as a parameter. We assume that bacteria are in a box of size L with reflecting walls and that they do not interact among each other. We focus on the steady-state behavior

of a population.

As a way to probe chemotactic accumulation, we consider a linear concentration profile of nutrient: $c(x) = cx$. For small α this gives rise to a linear steady-state distribution of individual bacterium position, or, equivalently, to a linear density profile of a bacterial population. Its slope, which we denote by β , is a measure of the strength of chemotaxis. A large slope indicates strong bacterial preference for regions with higher nutrient concentration. Conversely, a vanishing slope implies that bacteria are insensitive to the gradient of nutrient concentration and are equally likely to be anywhere along the line. We would like to understand the way in which the slope β depends on the different time-scales present in the system.

A. Results in the linear model with non-adaptive response kernels

Before considering the full non-linear problem with a bilobe response kernel, we study a simpler, linear model. The model is defined by Eqs. 1-4 but with $\phi(x) = x$. Apart from allowing for a simpler treatment, this linear problem will also help us in developing a clearer picture of the non-linear problem. In the linear case, the problem can be solved by superposing the solutions of simpler problems—namely, with delta-function response kernels—with suitable chosen coefficients. Thus, solving the problem with a singular response kernel amounts to a full solution and we focus here on this case.

In our simulations, we start from an arbitrary bacterium position inside a box of size L . Each time step has a duration dt , during which a running bacterium moves over a distance vdt . This distance corresponds to one lattice spacing in our model, in which a lattice is introduced because time is discretized. At the end of each time step, we compute the functional defined in Eq. 3; for a singular response kernel, $R(t) = \alpha\delta(t - \Delta)$, this takes the form $\alpha c[x(t - \Delta)]$, where $c[x(t - \Delta)]$ is the nutrient concentration experienced by the bacterium at time $t - \Delta$. At the end of each time step the bacterium either tumbles, with a probability $(1 - \alpha c[x(t - \Delta)]) dt/\tau_R$, or continues to move in the same direction. At every tumble, the velocity of the bacterium is reversed with a probability q . The system reaches the steady state over a time scale $\sim L^2$ and the bacterial density profile inside the box becomes linear. We focus on the slope, β , of this profile.

According to our numerical simulations, for $\alpha < 0$, β increases with Δ and saturates for

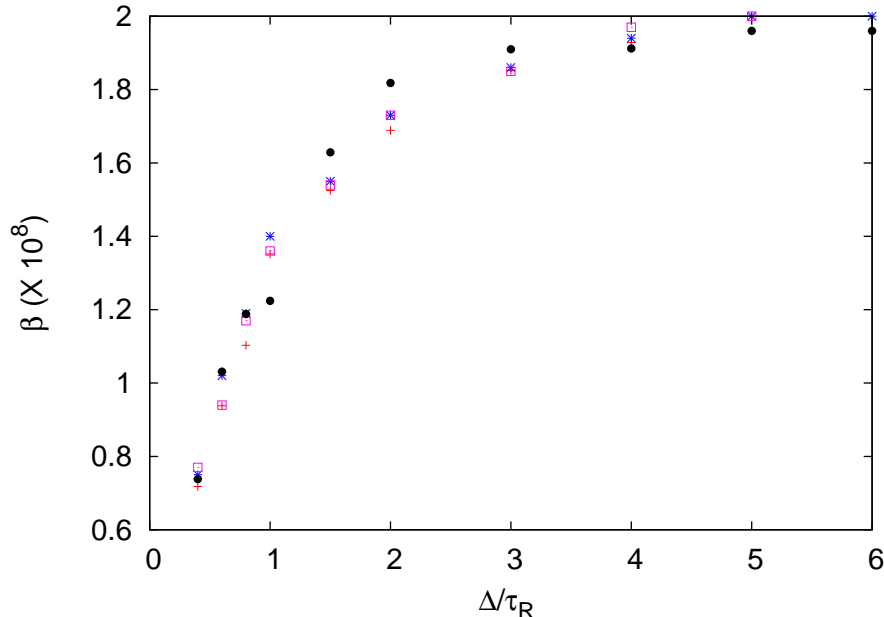


FIG. 2: The slope β as a function of Δ/τ_R , for the choice of response kernel $R(t) = \alpha\delta(t - \Delta)$. Note that for $\Delta \gg \tau_R$ the slope saturates to a non-vanishing value. The symbols +, *, and \square correspond to slopes measured in simulations with $\tau_R = 1.5, 1.0$, and 0.5 seconds, respectively. The black solid circles are derived from our coarse-grained formulation (Eq. 11). Here $q = 0.5$, $\alpha = -0.02$, $L = 1000\mu m$, $c = 0.001\mu m^{-1}$, $v = 10\mu m/s$.

$\Delta \gg \tau_R$ (Fig. 2). Simulations probing various values of τ_R also confirmed that $\beta = F(\Delta/\tau_R)$, i.e., that the slope is a scaling function of Δ/τ_R . Clearly, for positive α the sign of β is simply reversed, which corresponds to an unfavorable chemotaxis.

For small Δ , one can write down an approximate master equation for left-mover and right-mover densities and use it to show that the slope increases linearly with Δ (see the supporting information for details). It is surprising, however, that the slope saturates to a non-vanishing value for $\Delta \gg \tau_R$. Indeed one would expect that, if the response kernel relies on a point in time much earlier than $t - \tau_R$, a large enough number of tumbles occur between this past time and the present time so as to cancel any correlation between the nutrient concentration in the past and the present direction of motion. If this argument holds, one would expect that the slope β vanish for $\Delta \gg \tau_R$. Below, we return to this argument and explain why it is misleading.

B. Results in the linear model with adaptive response kernels

For wild-type bacteria, the total area under the response kernel vanishes (Fig. 1). As a result, their behavior is adaptive: chemotaxis is insensitive to the overall level of nutrient, but sensitive to spatial variations [8, 9]. In this section, before examining the case of a bilobe response kernel similar to the experimental one, we consider a toy model, defined by the difference of two singular forms: $R(t) = \alpha\delta(t - \Delta_1) - \alpha\delta(t - \Delta_2)$, with $\alpha > 0$. Because our problem is linear, the steady-state slope of bacterial density, β , can be calculated from a simple linear superposition, as:

$$\beta = F\left(\frac{\Delta_1}{\tau_R}\right) - F\left(\frac{\Delta_2}{\tau_R}\right). \quad (5)$$

Since the function $F(\cdot)$ is monotonic, the absolute value of β increases with the difference of Δ_1 and Δ_2 . Strong chemotaxis occurs when $\Delta_1 = 0$ and $\Delta_2 \gg \tau_R$.

We now turn to the experimental case of a bilobe response kernel. It is not computationally feasible to work with the complete set of experimental data [9]. So we have used a discrete subset (Fig. 1) which we represent as a series of delta-functions. Given this approximate response kernel, we investigate the behavior of the slope as a function of τ_R . Based on our results for the case of two delta functions, we expect that chemotaxis be weak if τ_R is either much smaller than the delay of the positive peak in the response kernel or much larger than the delay of the negative peak. We expect optimum chemotaxis for a value of τ_R that falls in between the two delays. We verify this prediction in Fig. 3 in the linear model. We note that the maximum slope occurs for a value of τ_R close to the experimentally recorded value of about 1s.

C. Results in the non-linear model

Experiments have established that bacteria modulate their run and tumble durations in response to a positive concentration gradient, but not to a negative one. In order to incorporate this feature in our model, we have to go beyond the linear response regime. In the non-linear model, whenever the linear functional (Eq. 3) is negative, the non-linear functional (Eq. 2) vanishes. This is the only difference with the linear model. Thus for a purely positive response kernel, the non-linear model behaves identically to a linear model, while for a purely negative response kernel, the non-linear model displays no chemotaxis

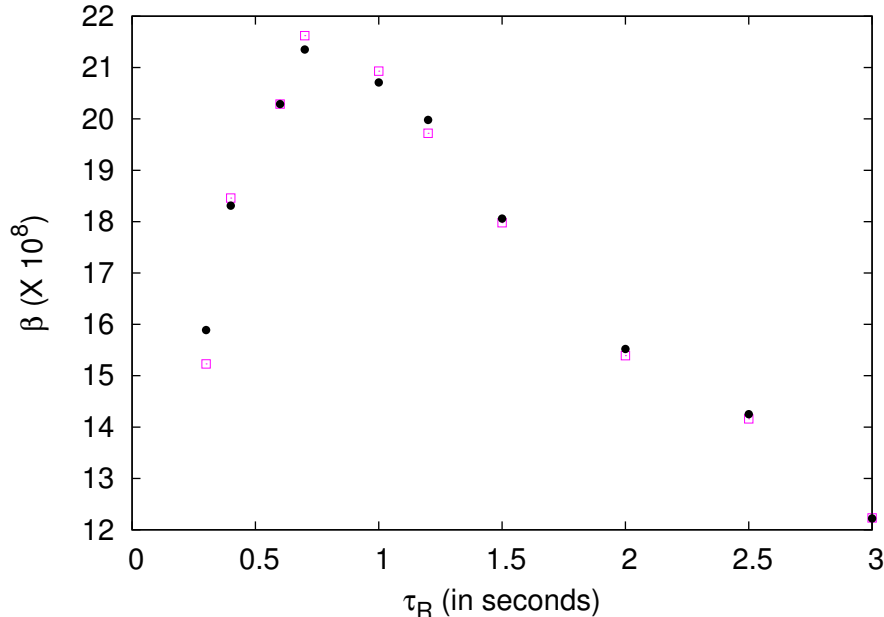


FIG. 3: The slope β as a function of τ_R for the experimental response kernel shown in Fig. 1. Open squares: numerical results from simulations. Solid circles: prediction of the coarse-grained model. Here, $q = 0.4$, $L = 1000\mu\text{m}$, $c = 0.0001\mu\text{m}^{-1}$, $v = 10\mu\text{m}/\text{s}$.

whatsoever. Hereafter, we examine only adaptive response kernels with balanced positive and negative contributions.

We first consider the idealized response kernel made of the superposition of positive and negative delta functions, $R(t) = \alpha\delta(t - \Delta_1) - \alpha\delta(t - \Delta_2)$. Simulations show that many qualitative features of the linear model still hold in the non-linear model. The scaling form valid in the linear case breaks down in the non-linear case, but the slope β increases with the separation between Δ_1 and Δ_2 and ultimately saturates to a non-vanishing value. Figures 4 and 5 display results of simulations. As expected, strong chemotaxis occurs when $\Delta_1 = 0$ and Δ_2 is substantially larger than τ_R . We have also verified that tumbling does not have much of an effect on the slope.

In the experimental case of a bilobe response kernel (Fig. 1), we find that strong chemotaxis occurs when τ_R lies between the positive and the negative peaks of the response kernel, as found in the linear case. For smaller or larger values of τ_R , chemotaxis becomes weak. Figure 6 illustrates our numerical results. We note that, again, the value of τ_R for which the slope is maximum falls close to the experimental value of about 1s .

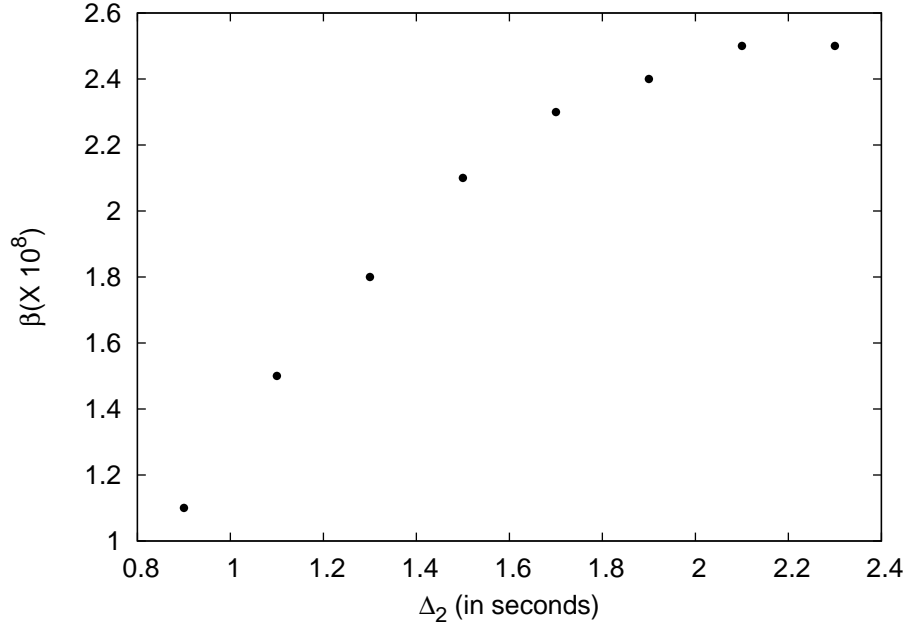


FIG. 4: The slope, β , as a function of Δ_2 , for $\Delta_1 = 0.5s$, in a non-linear model with balanced response kernel, $R(t) = \alpha\delta(t - \Delta_1) - \alpha\delta(t - \Delta_2)$. As in the linear model, β increases with the difference of Δ_1 and Δ_2 . Here, $\tau_R = 1$ sec, $q = 0.4$, $\alpha = 0.1$, $L = 1000\mu m$, $c = 0.001\mu m^{-1}$, $v = 10\mu m/s$.

IV. COARSE-GRAINED DESCRIPTION OF CHEMOTAXIS AS DIFFUSION WITH DRIFT

In order to gain insight into our numerical results, we developed a simple coarse-grained model of chemotaxis. For the sake of simplicity, we first present the model for a non-adaptive, singular response kernel, $R(t) = \alpha\delta(t - \Delta)$, and, subsequently, we generalize the model to adaptive response kernels by making use of linear superposition.

The memory trace embodied by the response kernel induces temporal correlations in the trajectory of the bacterium. However, if we consider the coarse-grained motion of the bacterium over a spatial scale that exceeds the typical run stretch and a temporal scale that exceeds the typical run duration, then we can assume that it behaves as a Markovian random walker with drift velocity V and diffusivity D . Since the steady-state probability

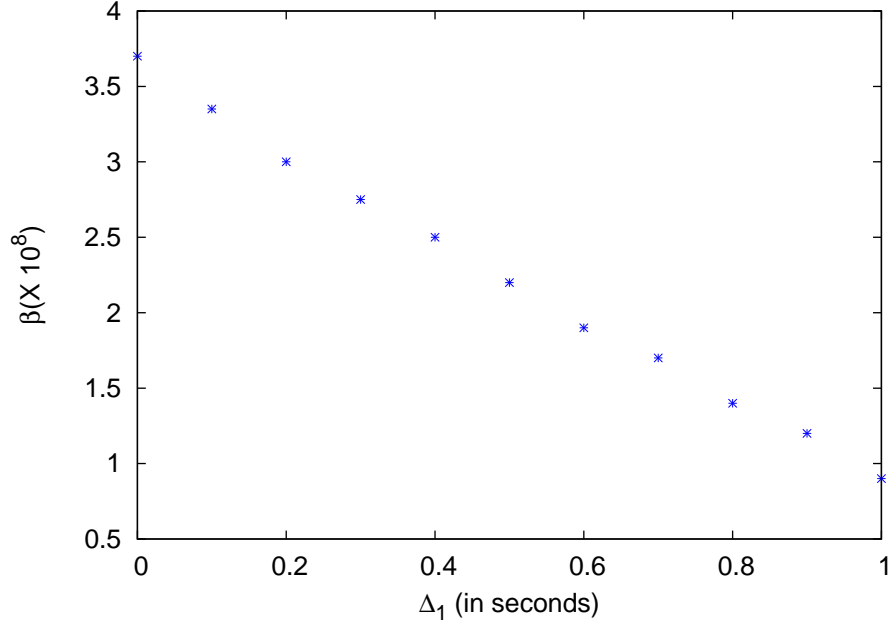


FIG. 5: The slope, β , as a function of Δ_1 , for $\Delta_2 = 1.5s$, in a non-linear model with balanced response kernel, $R(t) = \alpha\delta(t - \Delta_1) - \alpha\delta(t - \Delta_2)$. Numerical parameters are as in Fig. 4.

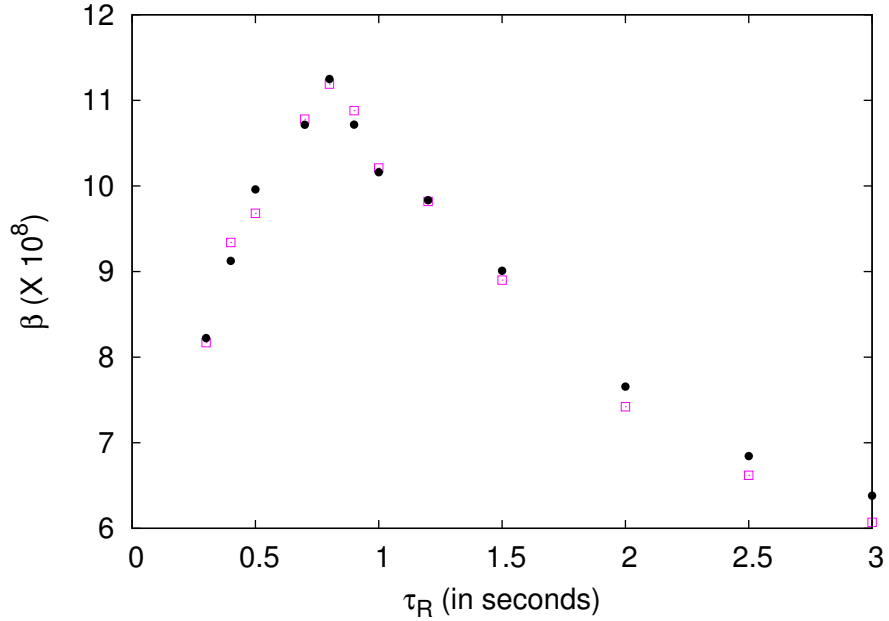


FIG. 6: The slope, β , as a function of τ_R , in a non-linear model with the experimental bilobe response kernel of Fig. 1. Open squares: numerical results from simulations. Solid circles: prediction of the coarse-grained model. Numerical parameters as in Fig. 3.

distribution, $P(x) = P(\Delta, \tau_R, x)$, is flat for $\alpha = 0$, for small α we can write

$$P = P_0 + \alpha \mathcal{P}(\Delta, \tau_R, x) + o(\alpha^2), \quad (6)$$

$$D = D_0 + \alpha \mathcal{D}(\Delta, \tau_R, x) + o(\alpha^2), \quad (7)$$

$$V = \alpha \mathcal{V}(\Delta, \tau_R, x) + o(\alpha^2). \quad (8)$$

Here, $P_0 = 1/L$ and $D_0 = v^2 \tau_R$. Note that V is the chemotactic drift velocity, which vanishes if $\alpha = 0$. It is defined as the mean displacement per unit time of a bacterium starting at a given location. Clearly, even in the steady state when the current J , defined through $\partial_t P = -\partial_x J$, is zero, V may be non-zero (see Eq. 10 below). In general, the non-Markovian dynamics make V dependent on the initial conditions. However, in the steady state this dependence is lost and V can be calculated, for example, by performing a weighted average over the probability of histories of a bacterium. This is the quantity that is of interest to us. An earlier calculation by de Gennes showed that, if the memory preceding the last tumble is ignored, then for a linear profile of nutrient concentration, the drift velocity is independent of position and takes the form $V = \alpha c v^2 \tau_R \exp(-\Delta/\tau_R)$ [10]. While the calculation applies in a regime with $\Delta \ll \tau_R$ (because of memory erasure), in fact its result captures the behavior well over a wide range of parameters (see Fig. 7). To measure V in our simulations, we compute the average displacement of the bacterium during one run duration in the steady state (as explained above), and we extract therefrom the drift velocity. (For details of the derivation, see the Supporting Information.) We find that V is negative for $\alpha < 0$ and that its magnitude falls off with increasing values of Δ (Fig. 7). We also verify that V indeed does not show any spatial dependence (data included in the Supporting Information).

To obtain the diffusivity, D , we first calculate the effective mean free path in the coarse-grained model. The tumbling frequency of a bacterium is $(1 - \alpha c x(t - \Delta))/\tau_R$ and depends on the details of its past trajectory. In the coarse-grained model, we replace the quantity $\alpha c x(t - \Delta)$ by an average $\alpha c \langle x(t - \Delta) \rangle$ over all the trajectories within the spatial resolution of the coarse-graining. Equivalently, in a population of non-interacting bacteria, the average is taken over all the bacteria contained inside a blob, and, hence, $\langle x(t - \Delta) \rangle$ denotes the position of the center of mass of the blob at a time $t - \Delta$ in the past. As mentioned above, the drift velocity is proportional to α , so that $\alpha c \langle x(t - \Delta) \rangle = \alpha c x(t) + O(\alpha^2)$. The average tumbling frequency then becomes $(1 - \alpha c x)/\tau_R$ and, consequently, the mean free path becomes $\tau_{MFP} = \tau_R/(1 - \alpha c x) \simeq \tau_R(1 + \alpha c x)$. As a result, the diffusivity is expressed

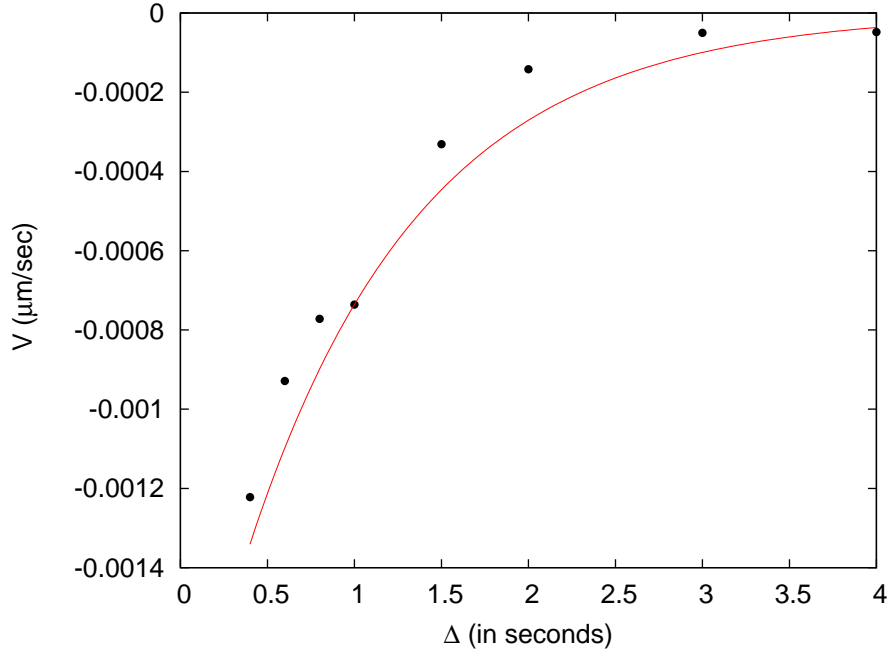


FIG. 7: The chemotactic drift velocity, V , as a function of Δ , for the response kernel $R(t) = \alpha\delta(t - \Delta)$. Solid circles: numerical results. Line: approximate analytical results from [10]. $\tau_R = 1$ s and other numerical parameters as in Fig. 2

as $D = v^2\tau_{MFP} = v^2\tau_R(1 + \alpha cx)$. We checked this form against our simulation data (Fig. 8).

Having evaluated the drift velocity, V , and the diffusivity, D , we now proceed to write down the continuity equation. For a biased random walker on a lattice, with position-dependent hopping rates $d^+(x)$ and $d^-(x)$ towards the right and the left, respectively, one has $V = a(d^+(x) - d^-(x))$ and $D = a^2(d^+(x) + d^-(x))/2$, where a is the lattice constant. In the continuum limit, the temporal evolution of the probability density is given by a probability current, as

$$\partial_t P = -\partial_x J, \quad (9)$$

where the current takes the form

$$J = VP - \partial_x(DP). \quad (10)$$

For reflecting boundary condition $J = 0$, in the steady state. This constraint yields a steady-state slope

$$\beta = \alpha \partial_x \mathcal{P} = \alpha \frac{P_0}{D_0} (\mathcal{V} - \partial_x \mathcal{D}) = \frac{\alpha \mathcal{V}}{Lv^2\tau_R} - \frac{\alpha c}{L} \quad (11)$$

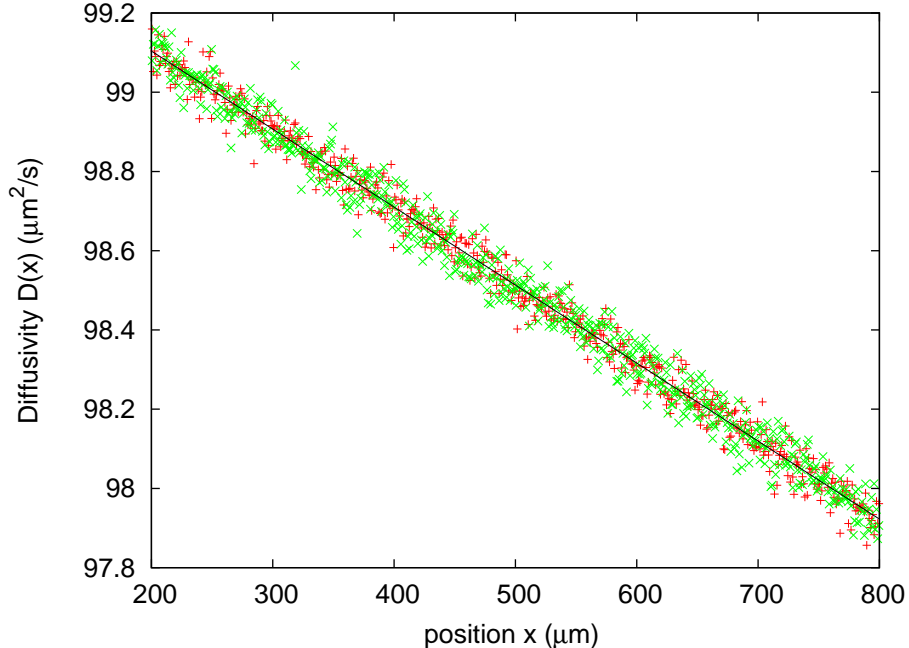


FIG. 8: The diffusivity, $D(x)$, as a function of position, x , for the response kernel, $R(t) = \alpha\delta(t-\Delta)$ with $\Delta = 1s$ (+) and $2s$ (x). $D(x)$ falls off linearly with x and is independent of Δ . Data fitting yields $D(x) = 99.5 - 0.00197x$ and the coarse-grained model predicts $D(x) = v^2\tau_R(1 + \alpha cx)$. For the chosen set of parameters, $v^2\tau_R = 100\mu m^2/s$ and the $v^2\tau_R\alpha c = -0.002$. The discrepancy between the numerical and the predicted slopes is due to higher-order corrections in α , while discretization of space in simulations causes the slight mismatch in the constant term. $\tau_R = 1s$ and other numerical parameters are as in Fig. 2.

for small α . We use our measured values for V and D (Figs. 7 and 8), and compute the slope using Eq. 11. (For details of the measurement of V see Supporting Information.) We compare our calculation with simulation results in Fig. 2, which exhibits close agreement.

According to Eq. 11, steady-state chemotaxis results from a competition between drift motion and diffusion. For $\alpha < 0$, the drift motion is directed toward regions with a lower nutrient concentration and hence opposes chemotaxis. Diffusion is spatially dependent and becomes small for large nutrient concentrations (again for $\alpha < 0$), thus increasing the effective residence time of the bacteria in favorable regions. For large values of Δ , the drift velocity vanishes and one has a strong chemotaxis with a saturation of bacterial accumulation as Δ increases (Fig. 2). Finally, for $\Delta = 0$, the calculation by de Gennes yields $V = \alpha cv^2\tau_R$ which exactly cancels the spatial gradient of D (up to linear order in α), and

there is no accumulation [10, 11].

These conclusions are easily generalized to adaptive response functions. For $R(t) = \alpha\delta(t - \Delta_1) - \alpha\delta(t - \Delta_2)$, within the linear response regime, the effective drift velocity and diffusivity can be constructed by simple linear superposition: The drift velocity reads $V = \alpha\mathcal{V}(\Delta_1) - \alpha\mathcal{V}(\Delta_2)$. Interestingly, the spatial dependence of D cancels out and $D = D_0 = v^2\tau_R$. The resulting slope then depends on the drift only and is calculated as

$$\beta = \frac{\alpha}{Lv^2\tau_R} (\mathcal{V}(\Delta_1) - \mathcal{V}(\Delta_2)). \quad (12)$$

In this case, the coarse-grained model is a simple biased random walker with constant diffusivity. For $\Delta_1 < \Delta_2$ and $\alpha > 0$, the net velocity, proportional to $\alpha(\mathcal{V}(\Delta_1) - \mathcal{V}(\Delta_2))$, is positive and gives rise to favorable chemotactic response, in which bacteria accumulate in regions with high food concentration. Moreover, the slope increases as the separation between Δ_1 and Δ_2 grows. We emphasize that there is no incompatibility between strong steady-state chemotaxis and large drift velocity. In fact, in the case of an adaptive response function, strong chemotaxis occurs only when the drift velocity is large.

For a bilobe response kernel, approximated by a superposition of many delta functions (Fig. 1), the slope, β , can be calculated similarly and in Fig. 3 we compare our calculation with the simulation results. We find close agreement in the case of a linear model with a bilobe response kernel and, in fact, also in the case of a non-linear model (Fig. 6).

V. DISCUSSION

We carried out a detailed analysis of steady-state bacterial chemotaxis in one dimension. The efficiency of the chemotaxis in the case of a linear concentration profile of the chemoattractant, $c(x) = cx$, was measured as the slope of the bacterium probability density profile in the steady state. For a singular impulse response kernel, $R(t) = \alpha\delta(t - \Delta)$, the slope was a scaling function of Δ/τ_R , which vanished at the origin, increased monotonically, and saturated at large argument. To understand these results we proposed a simple coarse-grained model in which bacterial motion was described as a biased random walk with drift velocity, V , and diffusivity, D . We found that D was independent of Δ and varied linearly with nutrient concentration. By contrast, V was spatially uniform and its value decreased monotonically with Δ and vanished for $\Delta \gg \tau_R$. We presented a simple formula for the

steady-state slope in terms of V and D . The prediction of our coarse-grained model agreed closely with our numerical results.

Further, we generalized the above results to the case of response kernels with arbitrary shapes in the linear model. For an adaptive response kernel, the spatial dependence of the diffusivity, D , cancels out but a positive drift velocity, V , ensures bacterial accumulation in regions with high nutrient concentration, in the steady state. In this case, the slope is directly proportional to the drift velocity. As the delay between the positive and negative peaks of the response kernel grows, the velocity increases, with consequent stronger chemotaxis.

Earlier studies of chemotaxis [14–17] put forth a coarse-grained model different from ours. In the model first proposed by Schnitzer for a single chemotactic bacterium [14], he argued that, in order to obtain favorable bacterial accumulation, tumbling rate and ballistic speed of a bacterium must both depend on the direction of its motion. In his case, the continuity equation reads

$$\partial_t P = \partial_x \left[\frac{\gamma_L v_R - \gamma_R v_L}{\gamma_L + \gamma_R} P - 2 \frac{v_R + v_L}{\gamma_R + \gamma_L} \partial_x \left(\frac{v_R v_L}{v_R + v_L} P \right) \right], \quad (13)$$

where $v_{L(R)}$ is the ballistic speed and $\gamma_{L(R)}$ the tumbling frequency of a bacterium moving toward the left (right). For *E. coli*, as discussed above, $v_L = v_R = v$, a constant independent of the location. In that case, Eq. 13 predicts that in order to have a chemotactic response in the steady state, one must have a non-vanishing drift velocity, *i.e.*, $(\gamma_L v_R - \gamma_R v_L)/(\gamma_L + \gamma_R) \neq 0$. This contradicts our findings for non-adaptive response kernels, according to which a drift velocity only hinders the chemotactic response. The spatial variation of the diffusivity, instead, causes the chemotactic accumulation. This is clearly not captured by Eq. 13. In the case of adaptive response kernels, the diffusivity became uniform while the drift velocity was positive, working in favor of chemotaxis. Comparing the expression of the flux, J , obtained from Eqs. 9 and 10 with that from Eq. 13, and matching the respective coefficients of P and $\partial_x P$, we find $D = 2v_R v_L/(\gamma_R + \gamma_L)$ and $V = (\gamma_L v_R - \gamma_R v_L)/(\gamma_L + \gamma_R)$. As we argued above in discussing the coarse-grained model for adaptive response kernels, both D and V are spatially independent. This puts strict restrictions on the spatial dependence of $v_{L(R)}$ and $\gamma_{L(R)}$. For example, as in *E. coli* chemotaxis, if $v_L = v_R = v$, then to recover our coarse-grained description, γ_L and γ_R must also be independent of x .

We comment on what is likely the possible origin of the discrepancy between our work and earlier treatments. In Ref. [14], a continuity equation was derived for the coarse-grained

probability density of a bacterium, starting from a pair of approximate master equations for the probability density of a right-mover and a left-mover, respectively. As the original process is non-Markovian, one can expect a master equation approach to be valid only at scales that exceed the scale over which spatiotemporal correlations in the behavior of the bacterium are significant. In particular, a biased diffusion model can be viewed as legitimate only if the (coarse-grained) temporal resolution allows for multiple runs and tumbles. If so, at a finer resolution than that of the coarse-grained model, left- and right-movers become entangled, and it is not possible to perform a coarse-graining procedure on the two species separately. Thus one cannot define probability densities for a left- and a right-mover that evolves in a Markovian fashion. In our case, left- and right-movers are coarse-grained simultaneously, and the total probability density is Markovian. Thus, our diffusion model differs from that of Ref. [14] because it resulted from a different coarse-graining procedure. The model proposed in Ref. [14] has been used extensively to investigate collective behaviors of *E. coli* bacteria such as pattern formation [15–17]. It would be worth asking whether the new coarse-grained description introduced shed a new light on bacterial collective behavior.

Acknowledgments

SC acknowledges the support from Lady Davis fellowship. RAdS was supported in part by the CNRS through UMR 8550.

-
- [1] H.C. Berg, *E. Coli in Motion* (Springer, New York, 2004).
 - [2] H.C. Berg and D.A. Brown *Nature* **239** 500 (1972).
 - [3] L. Turner, W.S. Ryu and H.C. Berg *J. Bacteriol* **182** 2793 (2000).
 - [4] The bacteria can also be repelled by chemorepellants and tend to accumulate in low chemical concentration. It is straightforward to reinterpret all our results and discussions for this case.
 - [5] M. Eisenbach *Mol. Microbiol.* **20** 903 (1996).
 - [6] N. Barkai and S. Leibler *Nature* **387** 913 (1997).
 - [7] U. Alon, M.G. Surette, N. Barkai and S. Leibler *Nature* **397** 168 (1999).
 - [8] S.M. Block, J.E. Segall and H.C. Berg, *Cell* **31** 215 (1982).

- [9] J.E. Segall, S.M. Block and H.C. Berg *Proc. Natl. Acad. Sci. USA* **83** 8987 (1986).
- [10] P.-G. de Gennes *Eur. Biophys. J.* **33** 691 (2004).
- [11] D.A. Clark and L.C. Grant *Proc. Natl. Acad. Sci. USA* **102** 9150 (2005).
- [12] Y. Kafri and R.A. da Silveira *Phys. Rev. Lett.* **100** 238101 (2008).
- [13] A. Celani and M. Vergassola *Proc. Natl. Acad. Sci. USA* **107** 1391 (2010).
- [14] M.J. Schnitzer *Phys. Rev. E* **48** 2553 (1993).
- [15] J. Tailleur and M.E. Cates *Phys. Rev. Lett.* **100** 218103 (2008); J. Tailleur and M.E. Cates *Eur. Phys. Lett.* **86** 60002 (2009).
- [16] N. Mittal, E.O. Budrene, M.P. Brenner and A. Oudenaarden *Proc. Natl. Acad. Sci. USA* **100** 13259 (2003).
- [17] A.G. Thompson, J. Tailleur, M.E. Cates and R.A. Blythe *J. Stat. Mech* P02029 (2011).

VI. SUPPORTING INFORMATION

A. Chemotaxis with non-vanishing tumbling durations

During a tumbling event the bacterium rotates about itself in a random fashion without any significant displacement. In a homogeneous nutrient concentration the average tumbling duration is $0.1s$, which is much smaller than the average run duration of $1s$. In the steady state one therefore expects that the bacterium spends only a fraction $\tau_T/\tau_R \simeq 0.1$ of the time in the tumbling state. For this reason, studies of chemotaxis often assume instantaneous tumbling.

It was shown recently that the existence of non-vanishing tumbling duration can yield interesting results: even with a punctual response kernel, $R(t) = \alpha\delta(t - \Delta)$ with $\Delta = 0$, *i.e.* a memoryless bacterium, one can observe a chemotactic response (Kafri *et al.*, 2008). Here, we provide a simplified derivation of the steady-state density profile in this Markovian limit. The result will prove useful also for the analysis of the non-Markovian case with $\Delta \neq 0$.

Let $L(x, t)$ and $R(x, t)$ be the density of left-movers and right-movers, respectively, at location x and time t . We denote by $T^R(x, t)$ and $T^L(x, t)$ the densities of tumblers that were moving to the right and left, respectively, before tumbling. For $\Delta = 0$, the time evolution of these quantities can be described by master equations. In the case in which both run and tumble durations are modulated, these read

$$\begin{aligned} \frac{\partial R(x, t)}{\partial t} = & -v\partial_x R(x, t) + (1 - q)T^R(x, t)\frac{(1+\alpha cx)}{\tau_T} \\ & + qT^L(x, t)\frac{1+\alpha cx}{\tau_T} - R(x, t)\frac{1-\alpha cx}{\tau_R}, \end{aligned} \quad (14)$$

$$\begin{aligned} \frac{\partial L(x, t)}{\partial t} = & v\partial_x L(x, t) + (1 - q)T^L(x, t)\frac{(1+\alpha cx)}{\tau_T} \\ & + qT^R(x, t)\frac{1+\alpha cx}{\tau_T} - L(x, t)\frac{1-\alpha cx}{\tau_R}, \end{aligned} \quad (15)$$

$$\frac{\partial T^R(x, t)}{\partial t} = R(x, t)\frac{1-\alpha cx}{\tau_R} - T^R(x, t)\frac{1+\alpha cx}{\tau_T}, \quad (16)$$

$$\frac{\partial T^L(x, t)}{\partial t} = L(x, t)\frac{1-\alpha cx}{\tau_R} - T^L(x, t)\frac{1+\alpha cx}{\tau_T}. \quad (17)$$

We consider perfectly reflecting boundary conditions at $x = 0$ and $x = L$. This means that in the steady state, we must have $R(x) = L(x)$. The steady-state total density at location

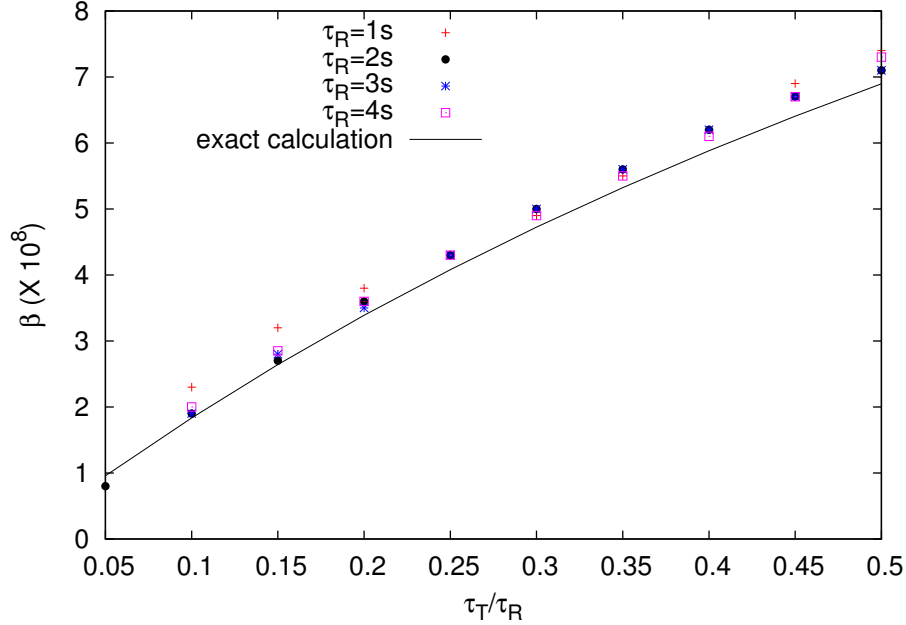


FIG. 9: The slope, β , as a function of τ_T/τ_R for $\Delta = 0$ and modulated tumbling. Simulation parameters are $L = 1000\mu m$, $\alpha = -0.1$, $q = 0.4$, $c = 0.001\mu m^{-1}$, $v = 10\mu m/s$.

x then becomes

$$\begin{aligned} N(x) &= R(x) + L(x) + T^R(x) + T^L(x) \\ &= \frac{1}{L(1+\frac{\tau_T}{\tau_R})} \left(1 + \frac{\tau_T}{\tau_R} \frac{1-\alpha cx}{1+\alpha cx} \right), \end{aligned} \quad (18)$$

For $\alpha cx \ll 1$, this expression is approximated by a linear dependence with the slope

$$\beta = G \left(\frac{\tau_T}{\tau_R} \right) = -\frac{2\alpha c \tau_T}{L \tau_R} \frac{1}{1 + \frac{\tau_T}{\tau_R} (1 - \alpha)}. \quad (19)$$

We compare our exact calculation with simulations in Fig. 9, which displays a systematic deviation for large argument. We have verified that the origin of this mismatch is the linearisation of Eq. 18.

For $\Delta \neq 0$ and when both runs and tumbles are modulated, we measure the density profile in numerical simulations. For $R(t) = \alpha\delta(t - \Delta)$, our numerics indicate that the steady-state slope, β , is a sum of the Markovian component, G , defined in Eq. 19, and a non-Markovian component, F , which depends on Δ/τ_R but is independent of τ_T :

$$\beta = F \left(\frac{\Delta}{\tau_R} \right) + G \left(\frac{\tau_T}{\tau_R} \right). \quad (20)$$

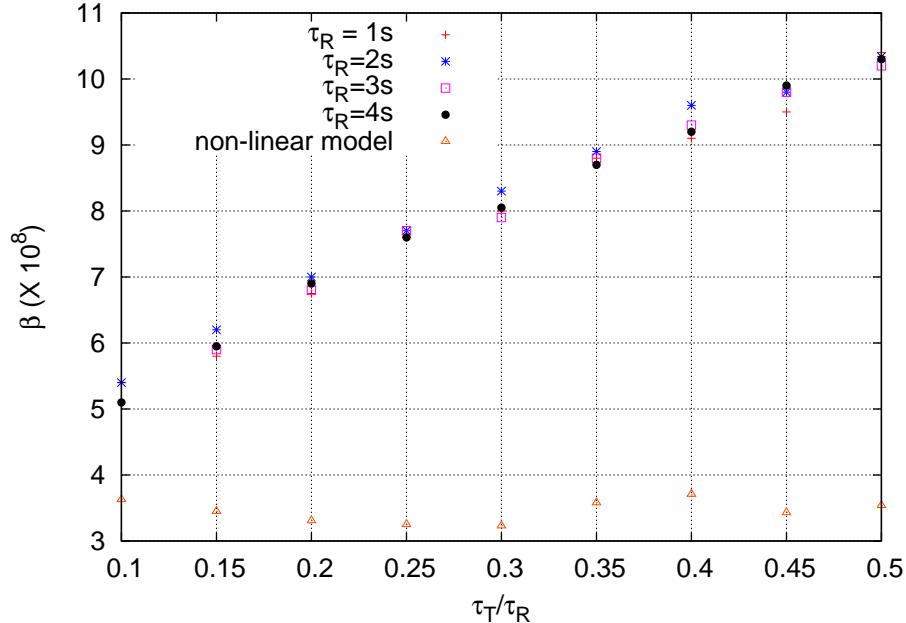


FIG. 10: The scaling collapse of the slope, β , as a function of τ_T/τ_R for fixed value of Δ/τ_R . We have used $\Delta/\tau_R = 0.5$ here. The other simulation parameters are as in Fig. 9. We also plot the slope, β , in the non-linear model with $R(t) = \alpha [\delta(t - \Delta_1) - \delta(t - \Delta_2)]$, $\Delta_1 = 0s$ and $\Delta_2 = 1.5s$ and $\tau_R = 1s$: β does not show any significant dependence on τ_T .

In Fig. 10, we exhibit this scaling form as a function of τ_T/τ_R for a fixed, non-vanishing value of Δ/τ_R . Our results suggests that β is made up of two contributions: one from the modulating runs, encoded in F , and one from non-instantaneous tumbles, encoded in G . The latter contribution is independent of Δ .

Finally, we can infer more general results from the simple form in Eq. 20. In particular, for an adaptive response function in the linear model, the positive and negative parts of the response function cancel out the effect of non-vanishing tumble durations. In this case, the steady-state slope, β , becomes independent of τ_T . Interestingly, we find the same applies even in the non-linear model (see Fig. 10).

B. Small-argument behavior of $F(\Delta/\tau_R)$

Here, we argue that for small Δ/τ_R the function $F(\Delta/\tau_R)$ is linear. First, note that for an impulse response kernel, $R(t) = \alpha\delta(t - \Delta)$ the tumbling probability during the interval

$[t, t + dt]$ is $[1 - \alpha c x(t - \Delta)] dt / \tau_R$. For small Δ , we can assume that no tumbling occurs during the interval $[t - \Delta, t]$. Then the effective tumbling rates become $[1 - \alpha c(x - v\Delta)] / \tau_R$ for right-movers and $[1 - \alpha c(x + v\Delta)] / \tau_R$ for left-movers. Based on this observation, we can write a pair of master equations that govern the densities of left-movers and right-movers, and we can solve them in the steady state. We obtain the slope, β , expressed as

$$\beta = -\frac{2\alpha c\Delta}{L\tau_R}. \quad (21)$$

Thus, in the limit $\Delta \ll \tau_R$ the scaling function $F(\Delta/\tau_R)$ depends linearly on its argument.

C. Chemotactic drift velocity as a function of position

Here, we show a sample of our numerical results on the drift velocity V as a function of position. We measure the average displacement of a bacterium in the steady state (see the corresponding discussion in the paper), and we compute V therefrom. Specifically, we perform the following procedure. Denote by $m_L(x)$ and $m_R(x)$, the total number of leftward and rightward runs, respectively, that initiate at the position x , over a certain time interval in the steady state. These quantities are well-defined in the context of our numerics because space is discretized. Furthermore, let $S_L(x)$ and $S_R(x)$ be the total leftward and rightward displacement, respectively, of the bacteria that undergo these runs. The average displacement per run is then given by $[S_R(x) - S_L(x)]/[m_R(x) + m_L(x)]$. Of course, the choice of the time scale as the duration of a run is arbitrary and other choices are equally valid. To leading order, this average displacement is linear in α . The drift velocity V , to order α , is then obtained by dividing this average displacement by τ_R . (Note that any $O(\alpha)$ correction to τ_R leads to $O(\alpha^2)$ correction to V , which we ignore here.) We find that up to the noise present in our numerical measurement, V does not display any dependence on position. An example is illustrated in Fig. 11.

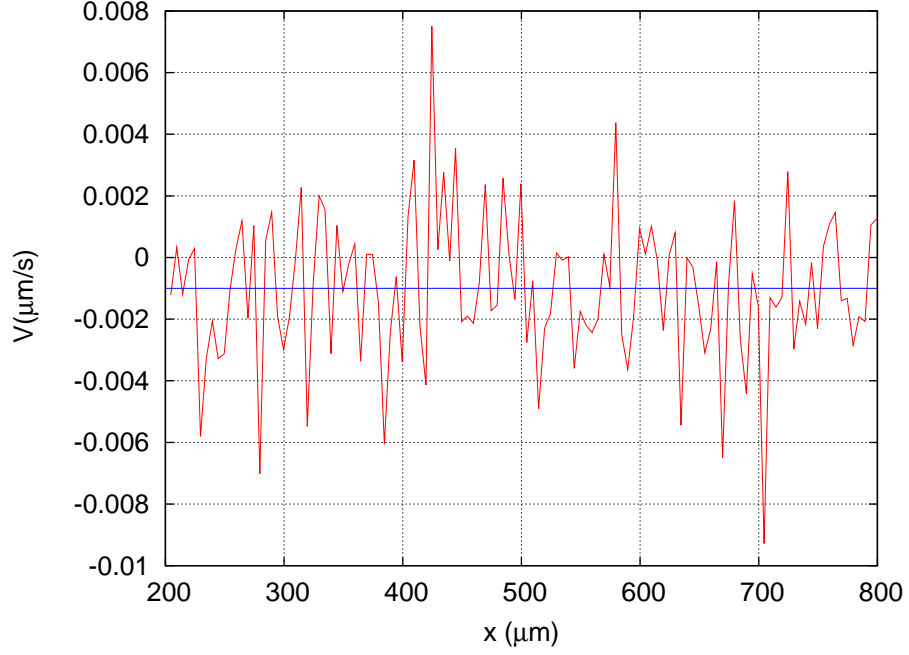


FIG. 11: Drift velocity, V , as a function of position, x , for the case of a singular response kernel $R(t) = \alpha\delta(t - \Delta)$ (red line). Here, $L = 1000\mu\text{m}$, $q = 1.0$, $\tau_R = 1\text{s}$, $\Delta = 1\text{s}$, $\tau_T = 0$, $v = 10\mu\text{m/s}$, $\alpha = -0.1$, $c = 0.001\mu\text{m}^{-1}$. Based on the data shown, the drift velocity is $0.001 \pm 0.0001\mu\text{m/s}$ (blue line).